Chapter 12

H9: Steady Flow through a Simple Channel Network

Contents

This problem was contributed by Peter E. Smith.

12.1 Problem Specification

H9 Steady flow through a simple channel network

Revised Problem H4 rectangular channels

Focus network connectivity, steady circulation.

The revised channels are rectangular, $\mathsf{SS} = 0$, and reach AB has been shortened to 24,000 ft. The network schematic remains unchanged, Figure 7.1. The complete channel geometry is listed in Table 12.1.

Open boundary conditions are fixed at

$$\eta_A(t) = +5 \text{ ft}, \quad Q_D(t) = 4,000 \text{ ft}^3/\text{s}, \quad Q_E(t) = 2,000 \text{ ft}^3/\text{s} \qquad \text{for all } t > 0 \qquad (12.1.1)$$

Reach	#1/AB	#2/BC	#3/CD	#4/BF	#5/FE	#6/CF
B ft	400	300	300	200	200	100
L ft	24,000	10,000	10,000	10,000	10,000	10,000
n	0.016	0.018	0.018	0.02	0.02	0.03
Node	A	B	C	D	E	F
Z ft	-20	-15	-10	+0	-5	-10

L is reach length.

Table 12.1: Channel geometry for Revised Schematic Network

Initial conditions at $t = 0$ are quiescence.

$$\eta(x, 0) = +5 \quad \text{ft}, \qquad Q(x, 0) = 0 \tag{12.1.2}$$

Use a fixed computational space step $\Delta x = 2,000$ ft and a fixed computational time step $\Delta t = 60$ s.

Compute and write to file in the STANDARD FORMAT the initial conditions at $t = 0$ and the model predictions for EVERY[1] time step to ONE HOUR PAST STEADY STATE.

12.2 Background

The CCW model is restricted to rectangular channels. The DWR model is restricted to a computational time step of 60 s. This problem provides an opportunity to compare all three models under exactly the same conditions.

12.3 Contra Costa Water District

Figures 12.1 and 12.2 shows the CCW-predicted η and Q evolution toward the steady state. The response patterns show the expected transient evolution through t_L = 60,000 s. The transient oscillations are initially strong and decay with time. By 30,000 s, steady state is approached, but not completely reached. The CCW data file has predictions through 180,000 s. At this time, the network flows are steady to three significant figures. The "truncation error" problems identified in Section 7.3 seem to have been resolved.

The gradually-varied water surface profile at t_L is shown in Figure 12.3. Visually, this is at steady state.

Figure 12.4 shows the instantaneous flow or mass balances at junctions B, C and F. The initiation and decay of the initial transients is evident. This is the expected response, mass being conserved at all three junctions.

Figures 12.1 though 12.4 are the expected response.

[1]The time to steady state is about twenty hours. The data files are very large and surface plots are very dense. For the following presentations, data file entries every 300 s to 60,000 s have been plotted.

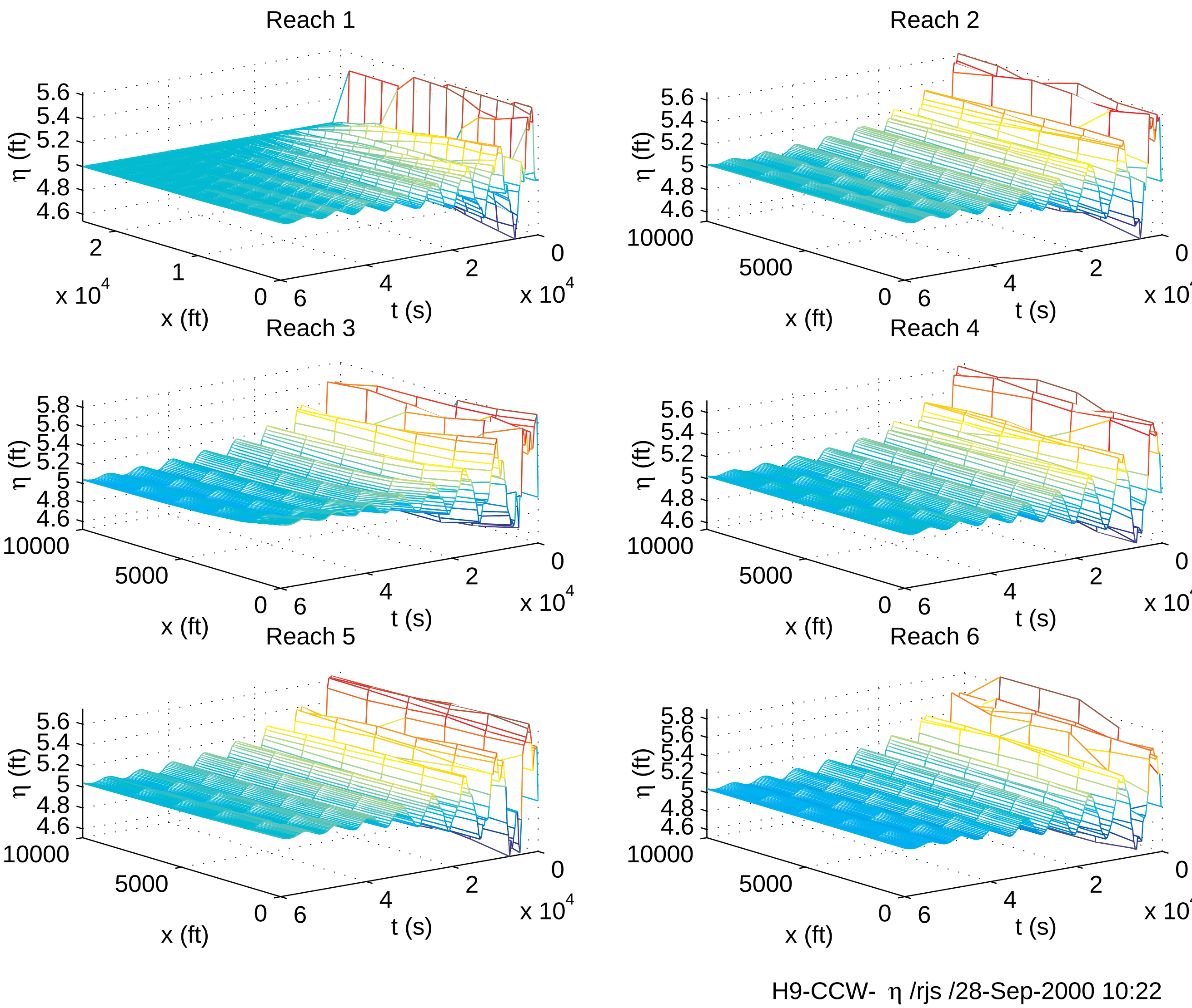

Figure 12.1: H9 CCW-predicted η solution field evolution.

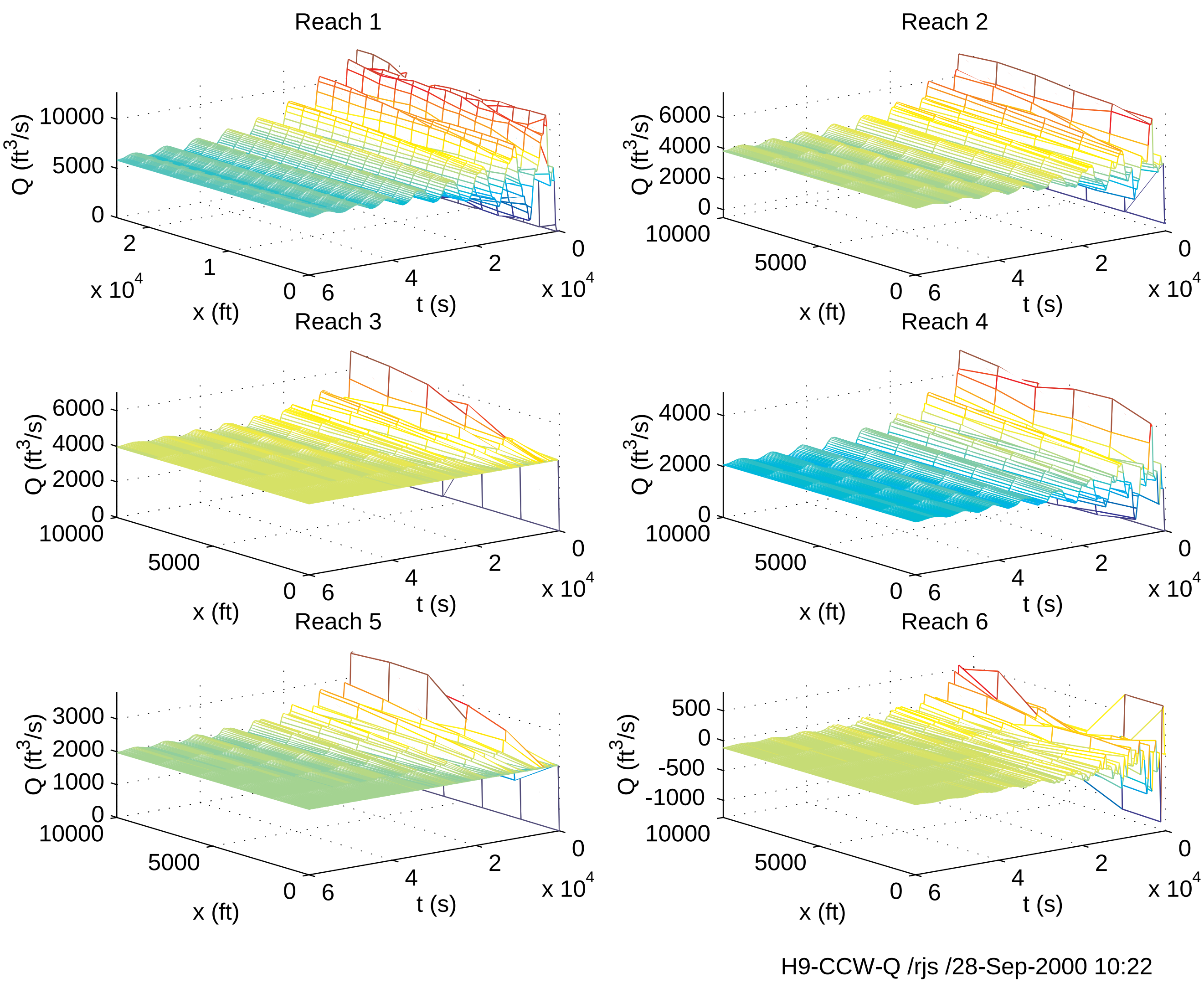

Figure 12.2: H9 CCW-predicted Q solution field evolution.

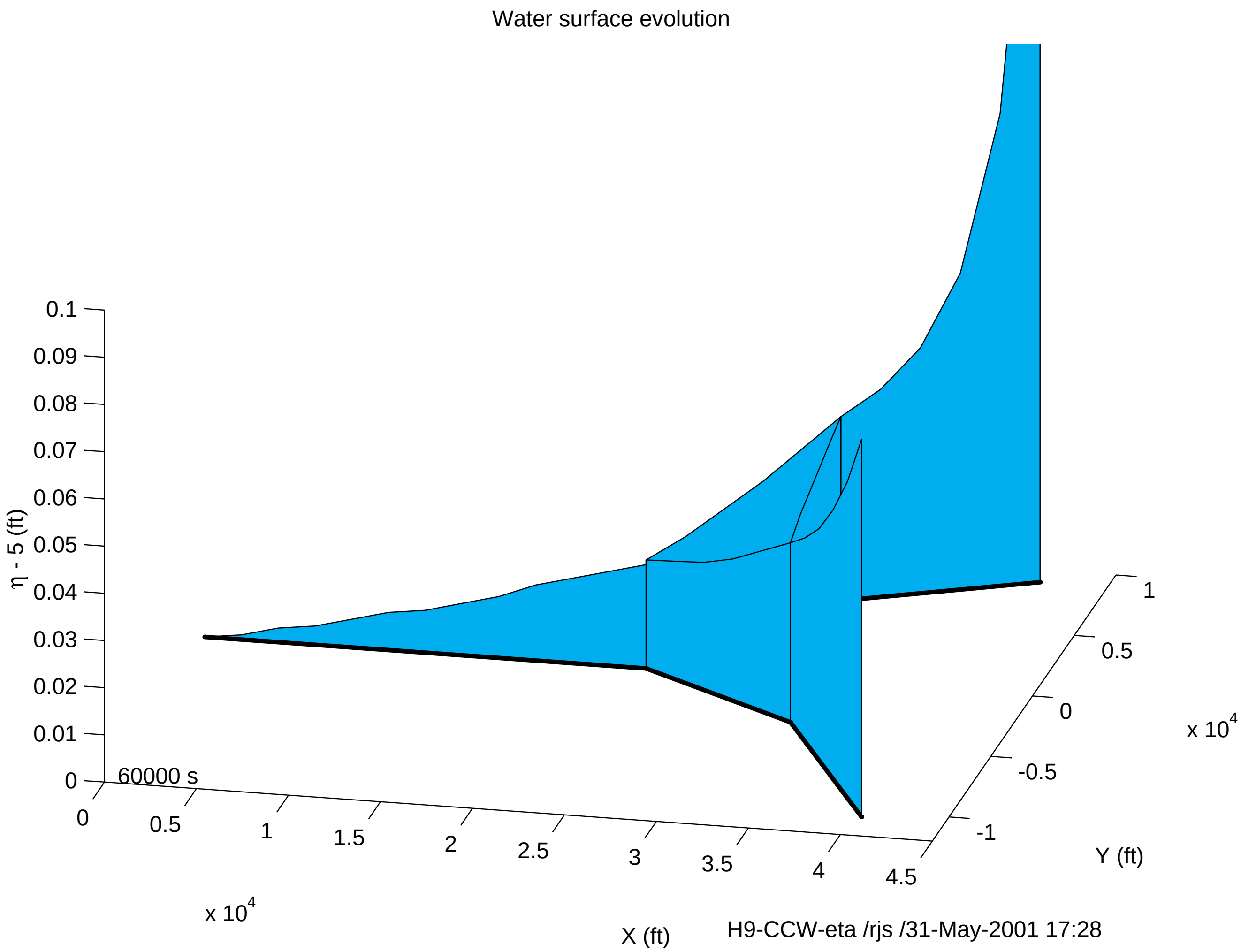

Figure 12.3: H9 CCW-predicted $\eta(x, t_L)$ solution field at $t_L = 30{,}000$ s.

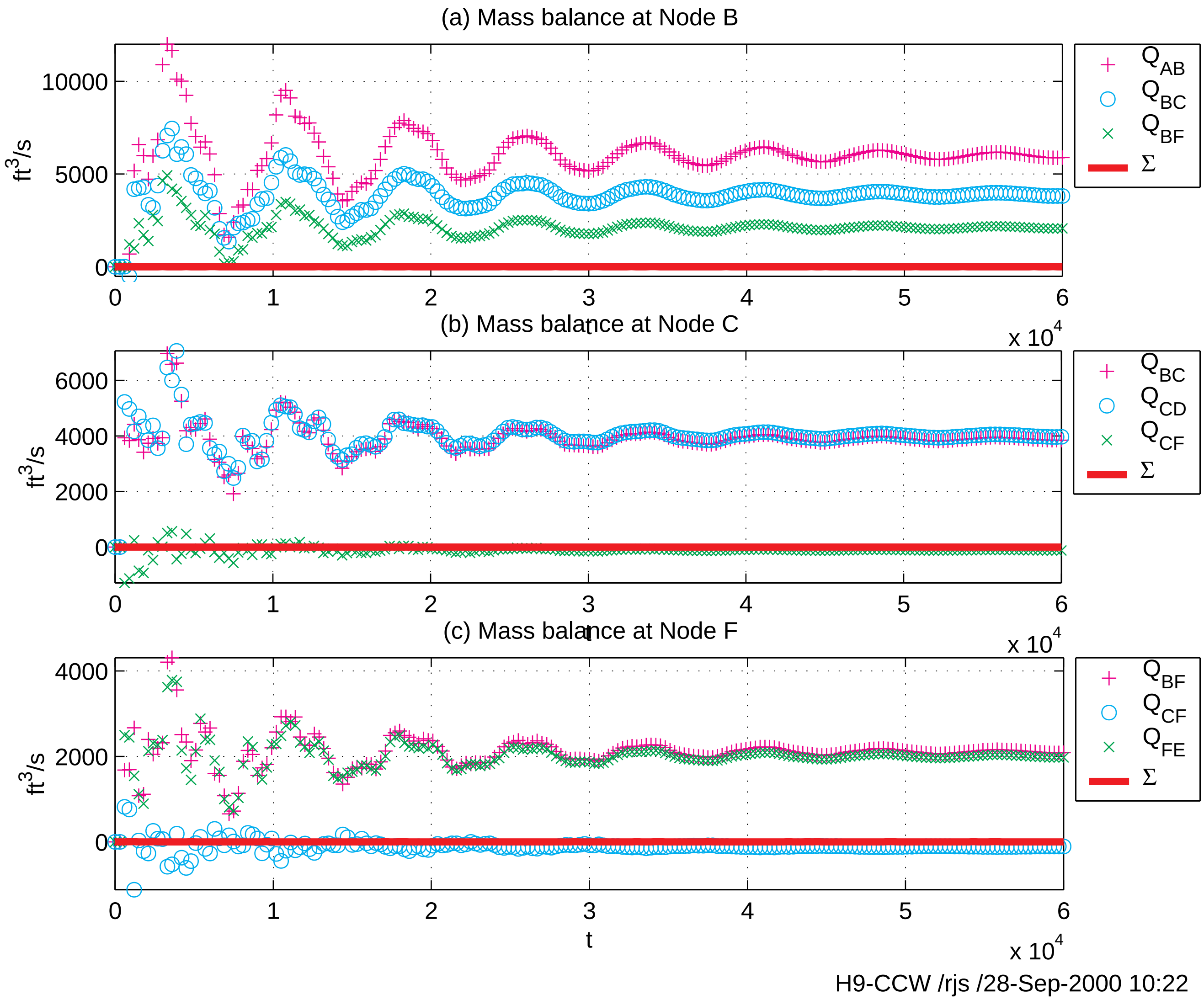

Figure 12.4: H9 CCW-predicted mass balances at network nodes.

12.4 Department of Water Resources

Figures 12.5 and 12.6 shows the DWR-predicted[2] η and Q evolution toward the steady state. The response patterns show the expected transient evolution through $t_L = 60{,}000$ s. The transient oscillations are initially strong and decay with time. By 30,000 s, steady state is approached, but not completely reached. The DWR data file has predictions through 3,599 s. With the time step correction, this is 215,940 s. At this time, the network flows are steady to six significant figures.

The gradually-varied water surface profile at t_L is shown in Figure 12.7. Visually, this is at steady state.

Figure 12.8 shows the instantaneous flow or mass balances at junctions B, C and F. The initiation and decay of the initial transients is evident. This is the expected response, mass being conserved at all three junctions.

Figures 12.5 though 12.8 are the expected response.

[2]The DWR data file reports the computational time step Δt as 1 s; it was apparently the specified 60 s. The time step has been changed to 60 s for the following analyses. The x axes are also directed in the wrong direction.

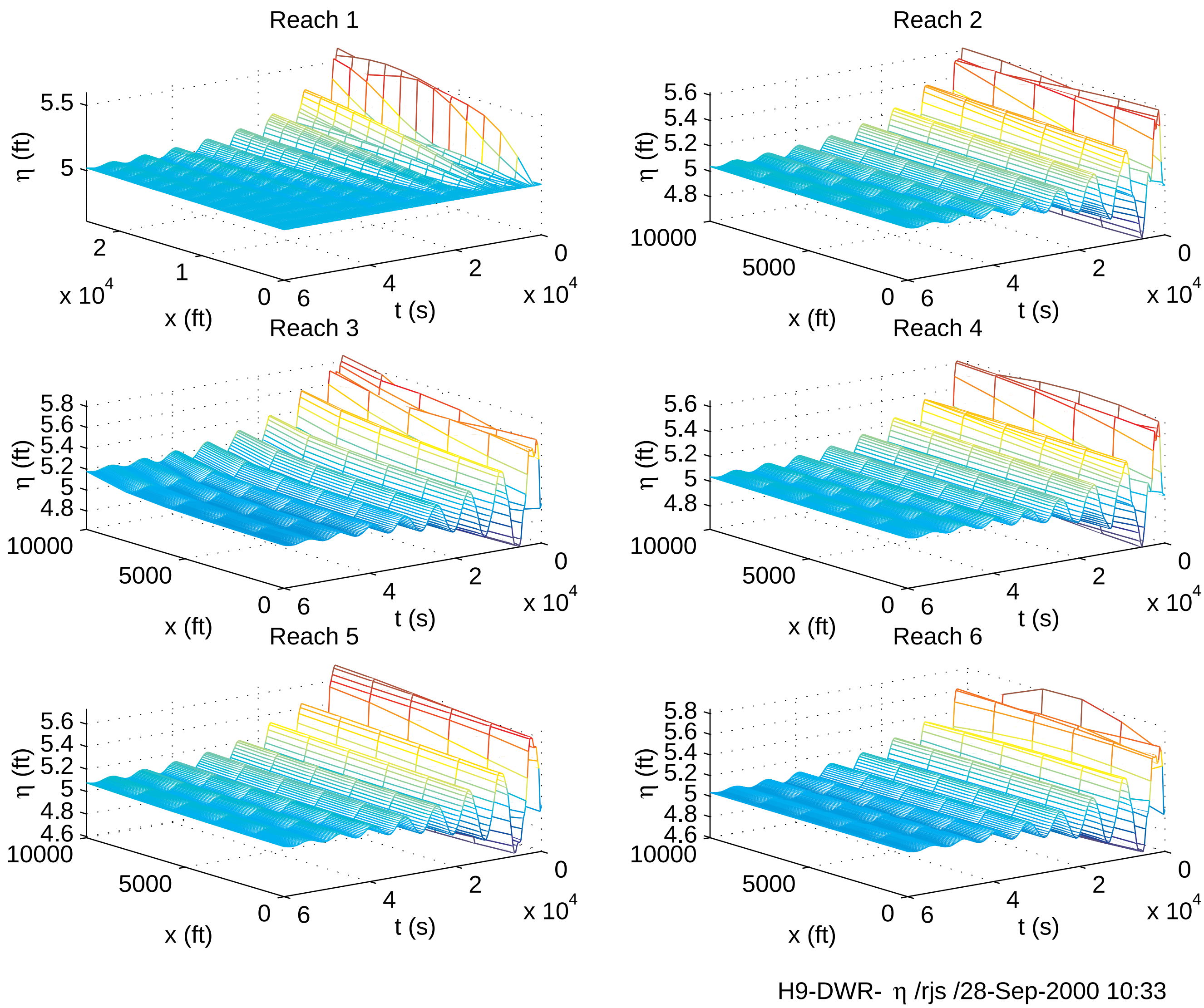

Figure 12.5: H9 DWR-predicted η solution field evolution.

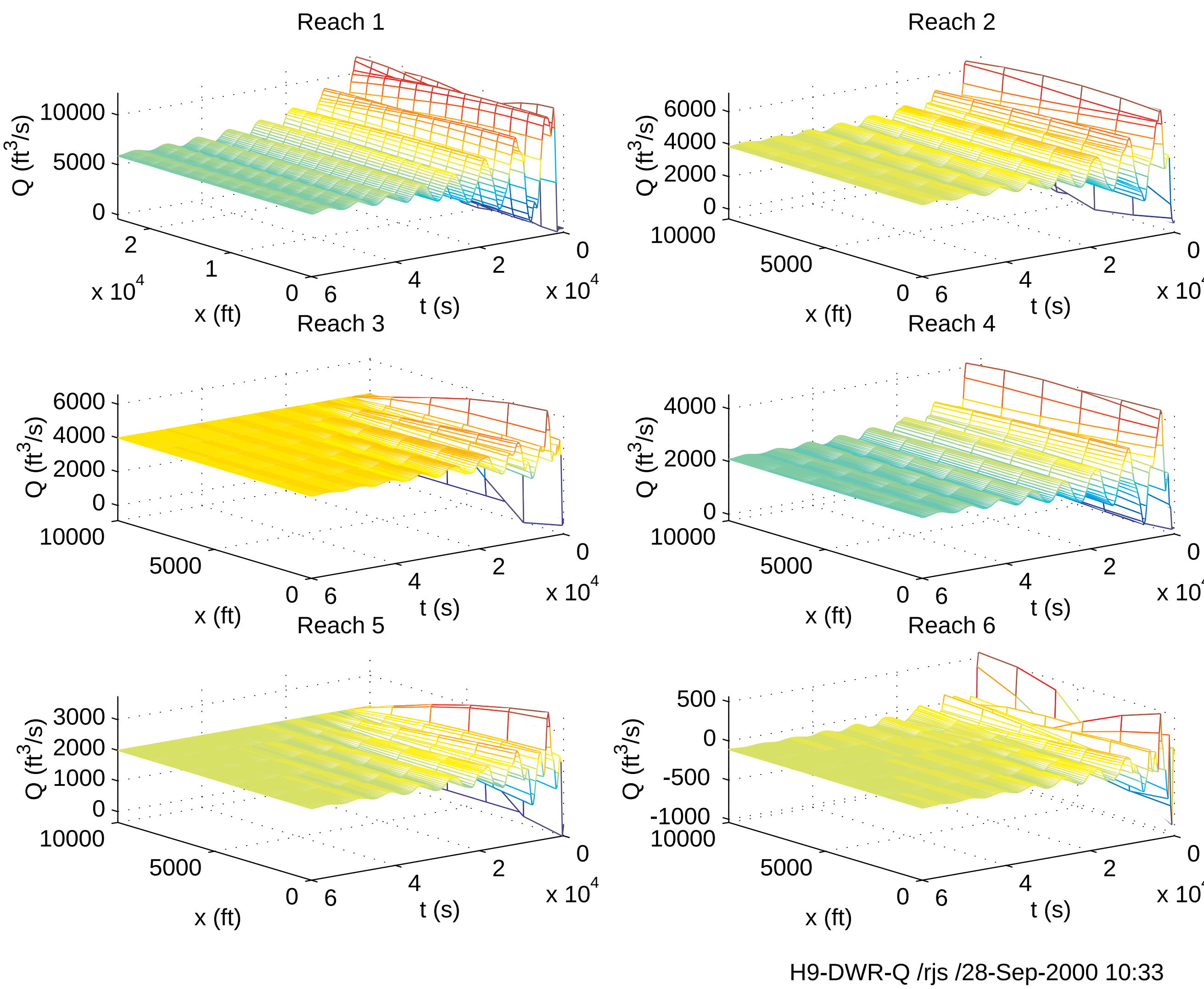

Figure 12.6: H9 DWR-predicted Q solution field evolution.

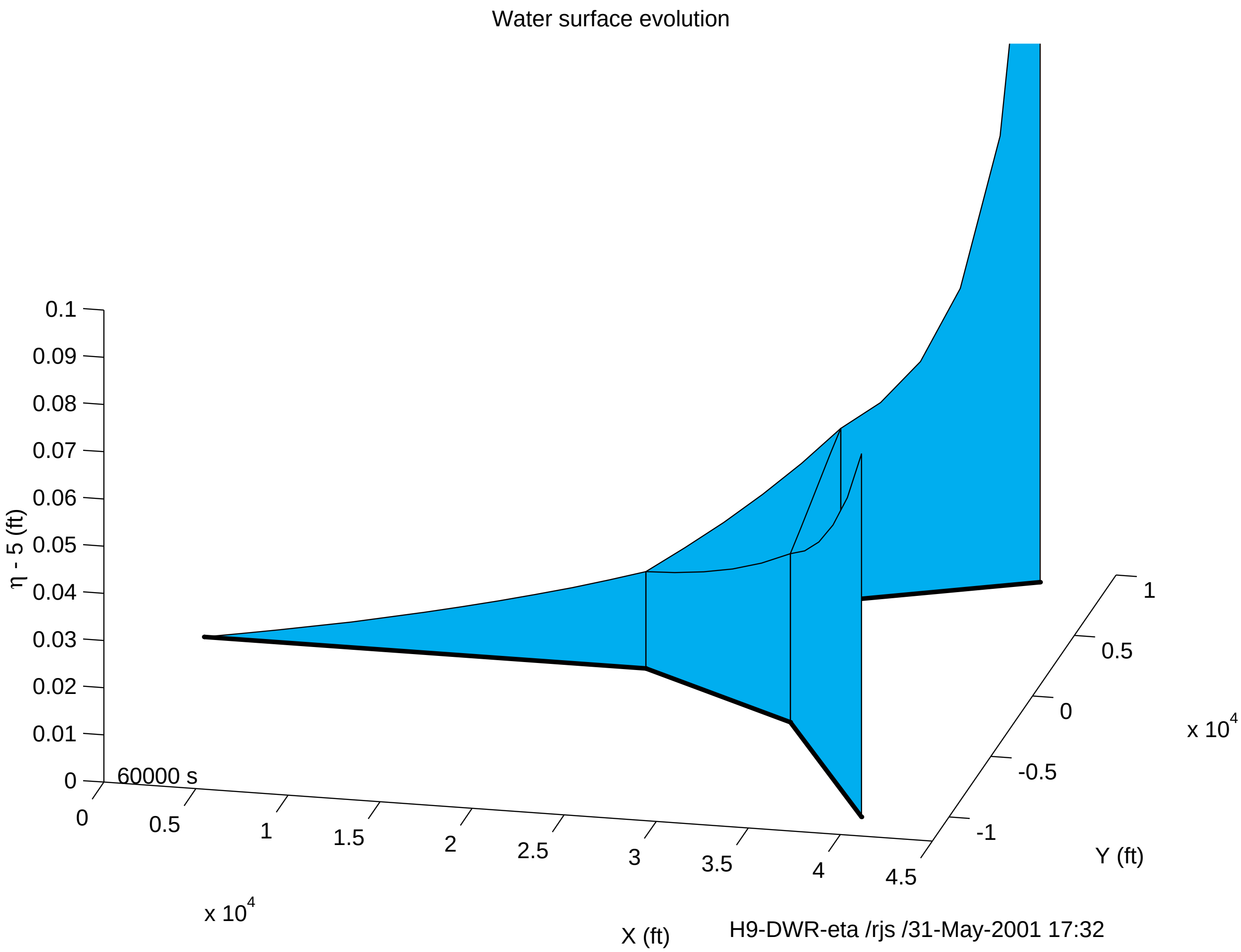

Figure 12.7: H9 DWR-predicted $\eta(x, t_L)$ solution field at $t_L = 30{,}000$ s.

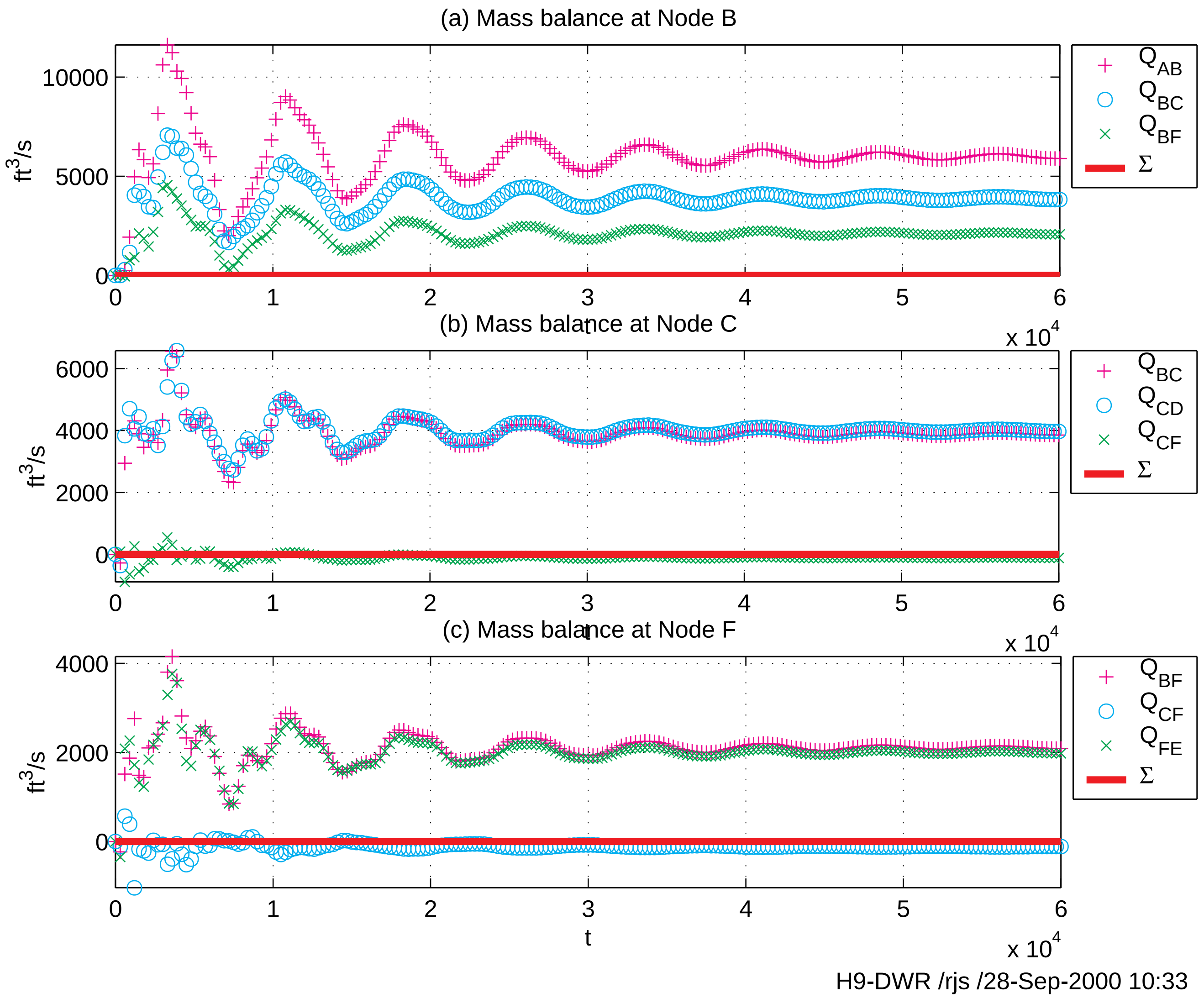

Figure 12.8: H9 DWR-predicted mass balances at network nodes.

12.5 Resource Management Associates

Figures 12.9 and 12.10 shows the RMA-predicted[3] η and Q evolution toward the steady state. The response patterns show the expected transient evolution through $t_L = 60{,}000$ s. The transient oscillations are initially strong and decay with time. By 30,000 s, steady state is approached, but not completely reached. The RMA data file has predictions through 180,000 s. At this time, the network flows are steady to three significant figures.

The gradually-varied water surface profile at t_L is shown in Figure 12.11. Visually, this is at steady state.

Figure 12.12 shows the instantaneous flow or mass balances at junctions B, C and F. The initiation and decay of the initial transients is evident. This is the expected response, mass being conserved at all three junctions.

Figures 12.9 though 12.12 are the expected response.

[3]RMA have used the specified Δx of 2,000 ft only in reach 1 (AB). They have used $\Delta x = 1{,}000$ ft for reaches 2 through 6.

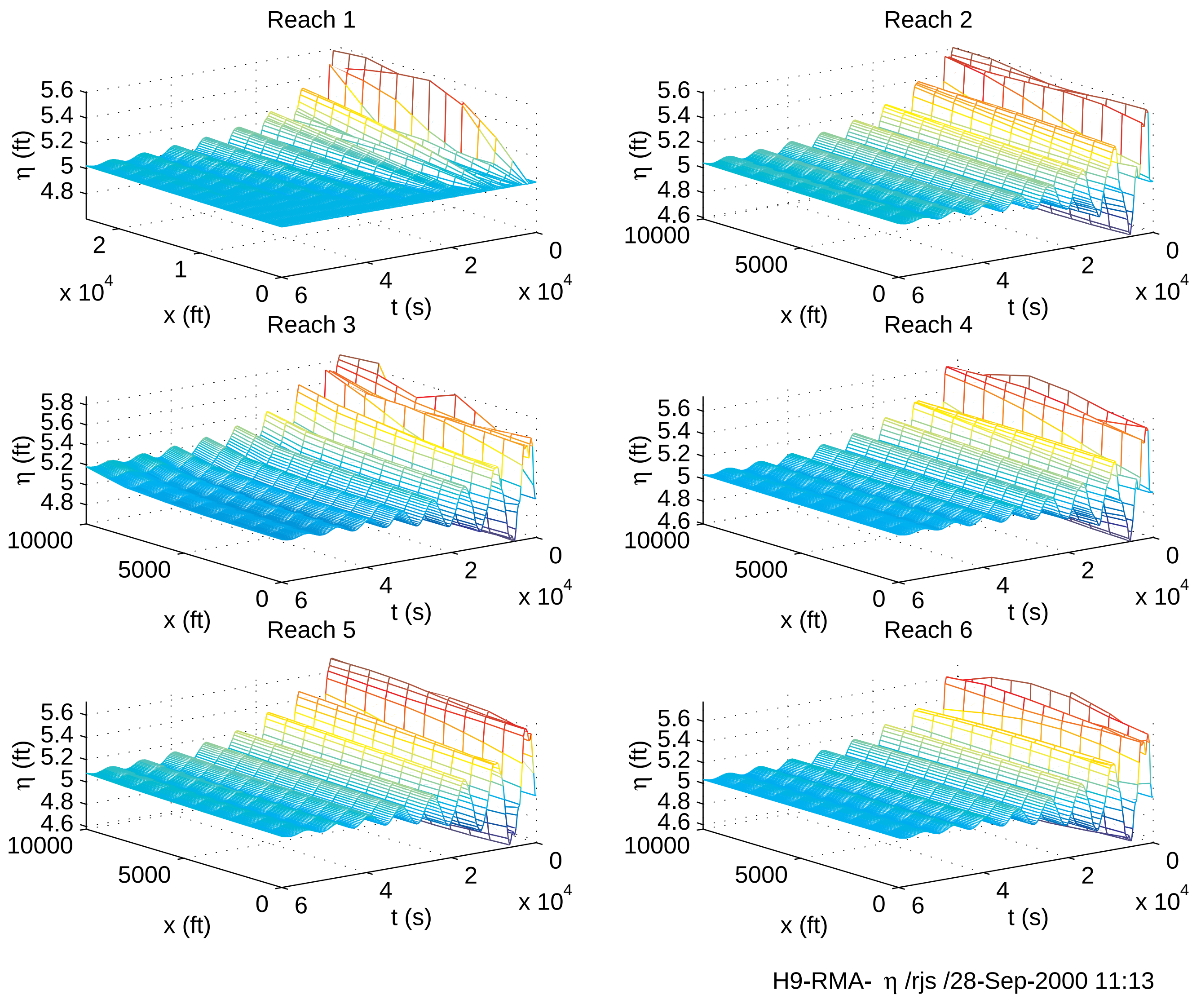

Figure 12.9: H9 RMA-predicted η solution field evolution.

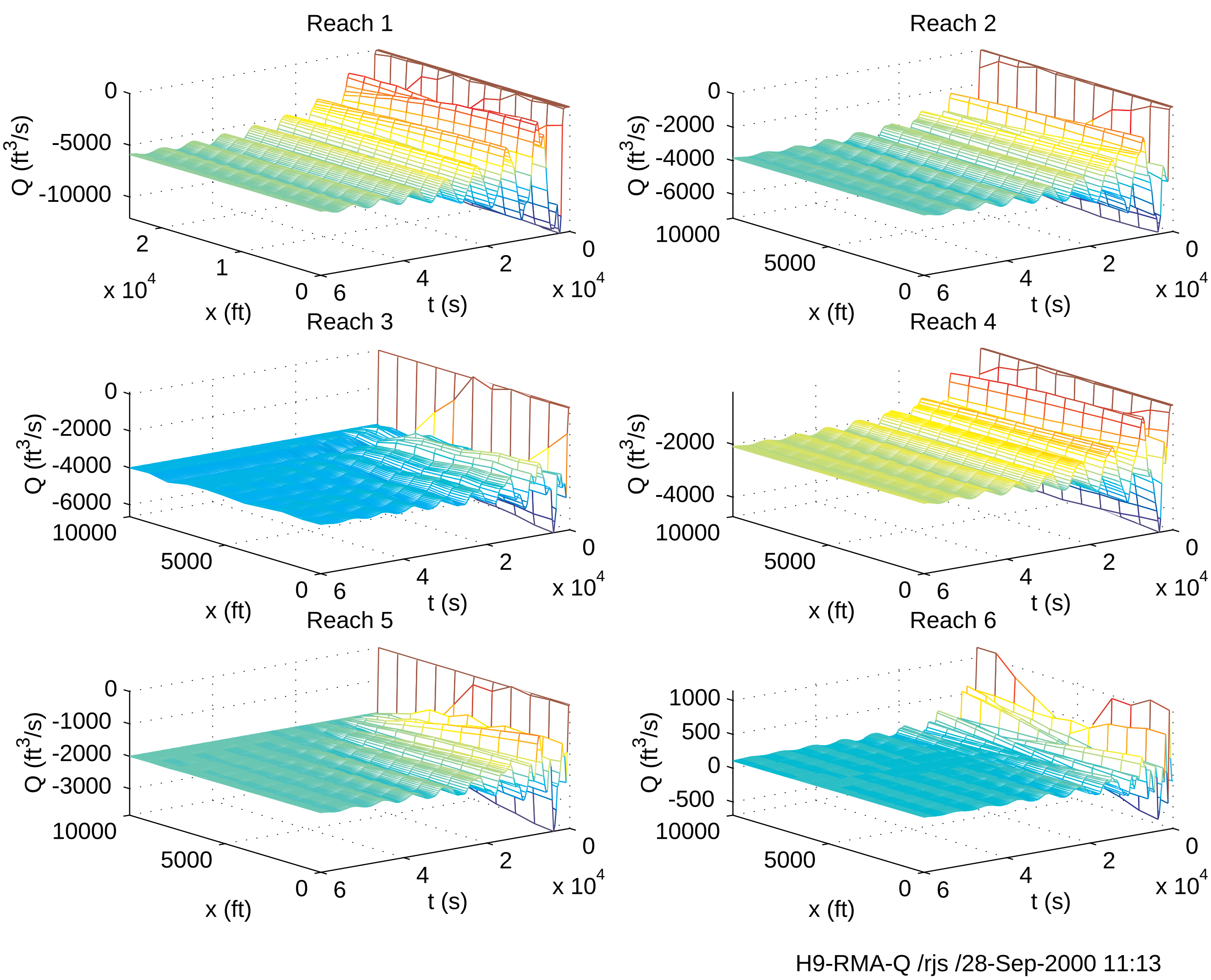

Figure 12.10: H9 RMA-predicted Q solution field evolution.

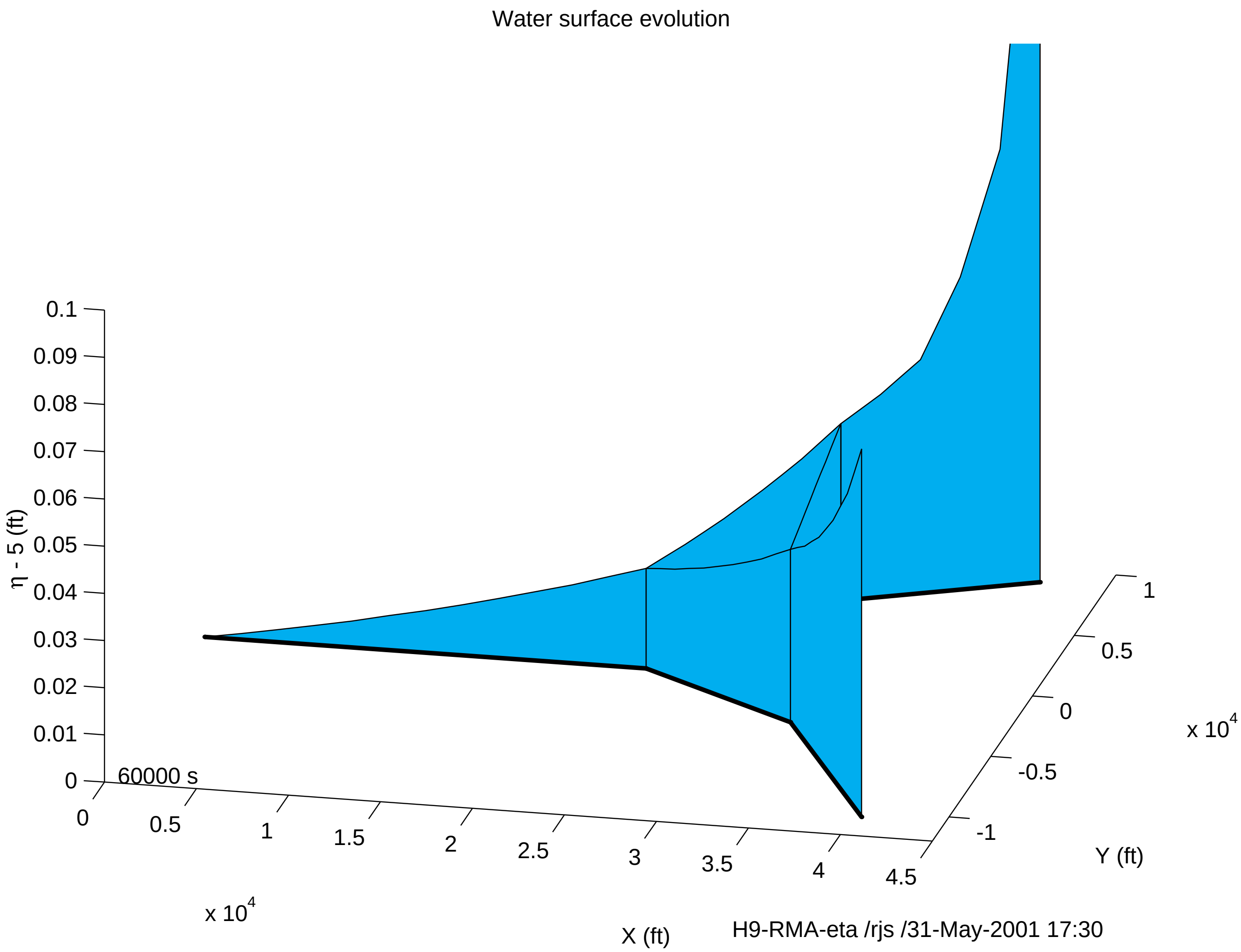

Figure 12.11: H9 RMA-predicted $\eta(x, t_L)$ solution field at $t_L = 30{,}000$ s.

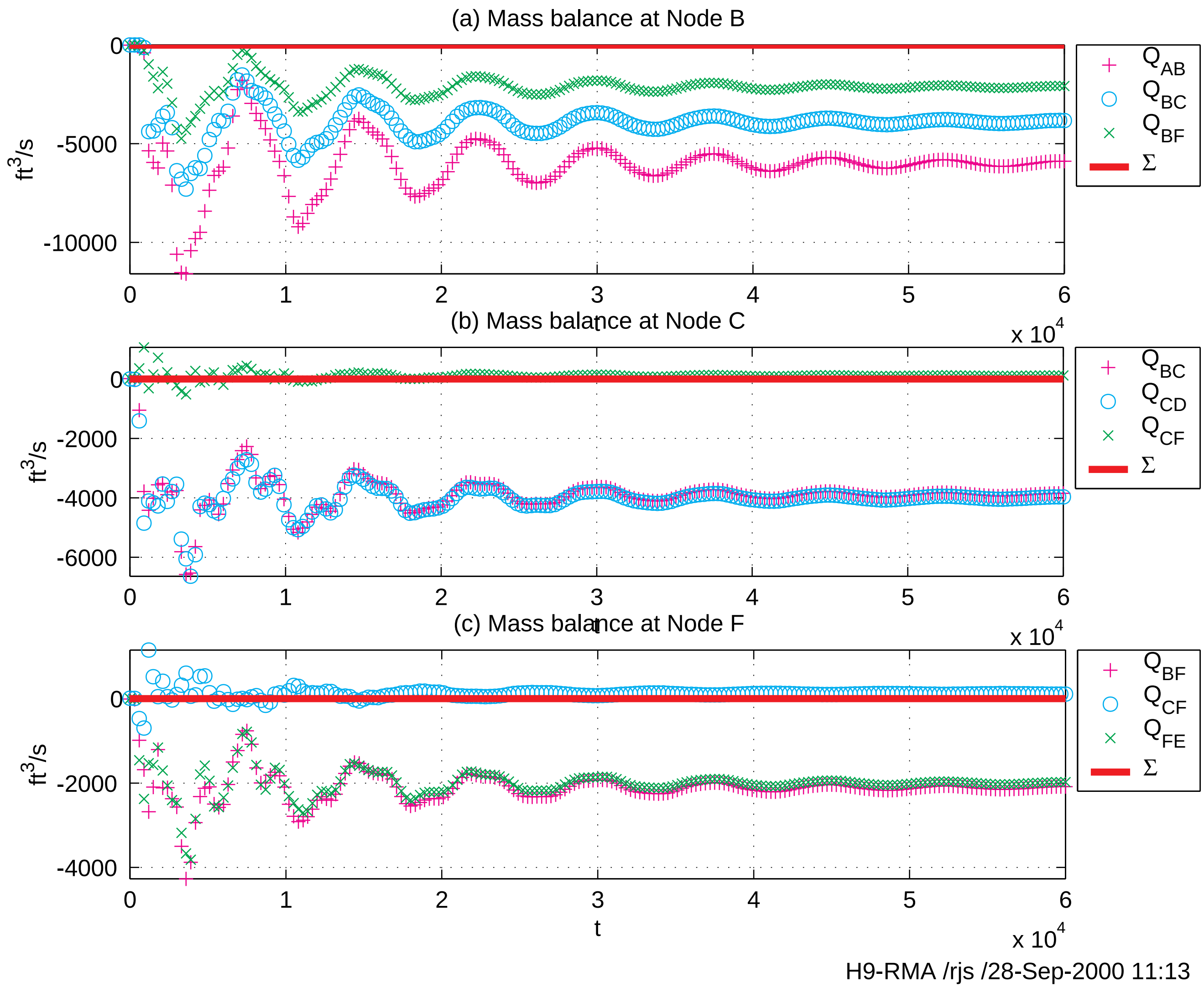

Figure 12.12: H9 RMA-predicted mass balances at network nodes.

12.6 Response Comparisons

The CCW model is restricted to rectangular channels. The DWR model is restricted to a computational time step of 60 s. This problem, a revision of H4, provides an opportunity to compare all three models under exactly the same conditions.

The most sensitive network link is CF/Reach 6. Figure 12.13a shows the CCW-predicted, DWR-predicted and RMA-predicted water surface evolutions at nodes C and F. Part (b) shows a time-expanded trace for the initial 15,000 s. Part (c) shows a time-expanded trace for the final 15,000 s. The general impression of the part (a) traces at C and F is excellent agreement. Free mode oscillations have been initiated by the initial conditions, and these decay slowly with friction. The shorter period modes are poorly resolved by the finite time resolution, and are also more strongly influenced by the implicit numerical filtering of the respective algorithms. This is seen most clearly in the part (b) time-expanded traces.

The steady state has been approached but not reached. The excellent asymptotic agreement is confirmed in the part (c) time-expanded traces, which have been offset for visibility. There is excellent magnitude agreement here, though a small phase difference between the CCW trace and the other two. The phase difference would seem to be a direct consequence of numerical filtering by the respective algorithms near the Nyquist limit.

Figure 12.14 shows the CCW-predicted, DWR-predicted and RMA-predicted flow evolution at nodes C and F within Reach CF/6. The story here is very similar to the η traces in Figure 12.13. There is excellent asymptotic agreement, except where the response is perhaps time-resolution challenged. The CCW response in the approximate anti-phase with the other two, but this is driven by the immediate response of the numerical algorithm to the initial excitation and is not especially significant.

In summary, these results follow the expected pattern. There is no suggestion that this is other than an excellent result for all three algorithms.

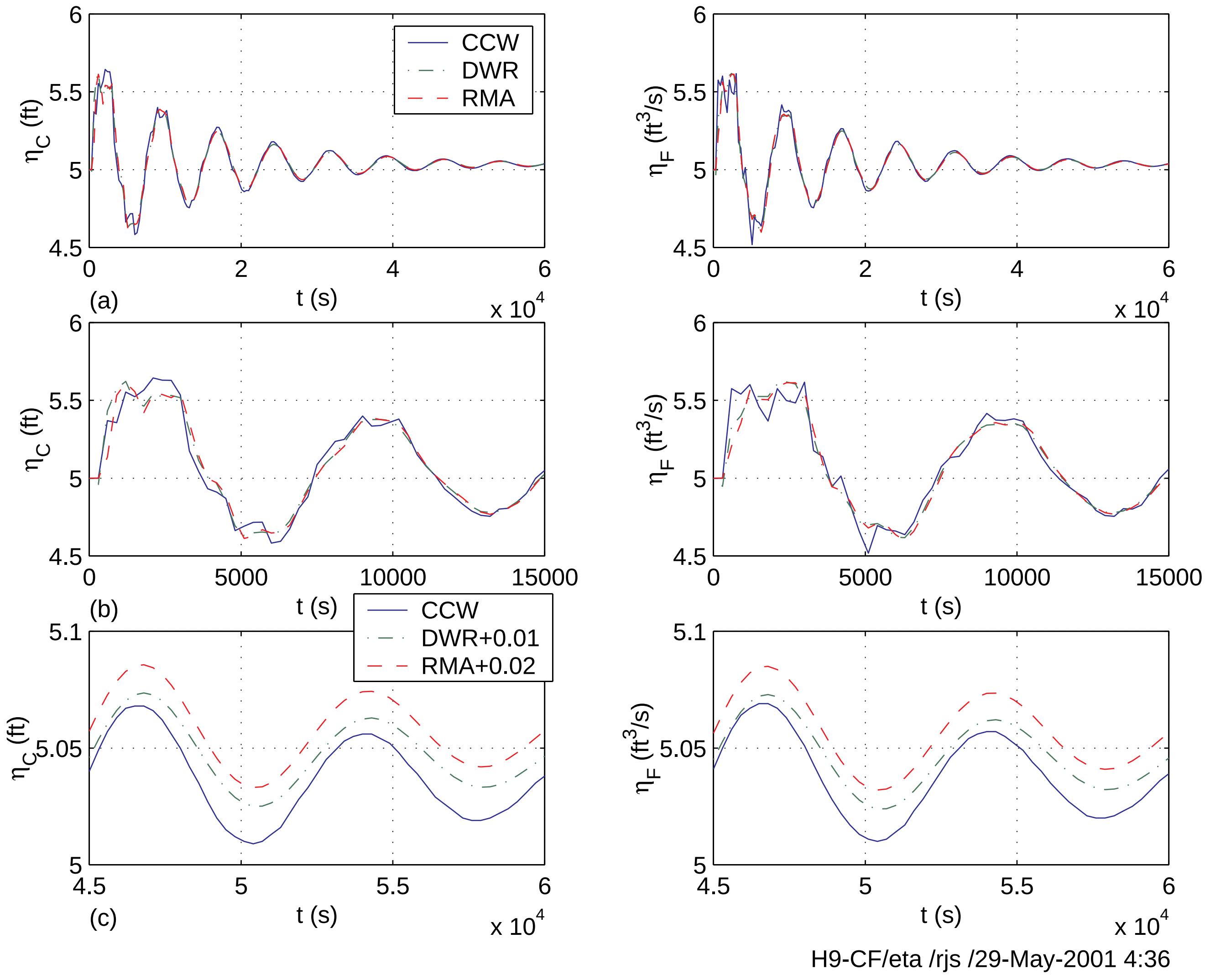

Figure 12.13: Water surface evolution at Nodes C and F.

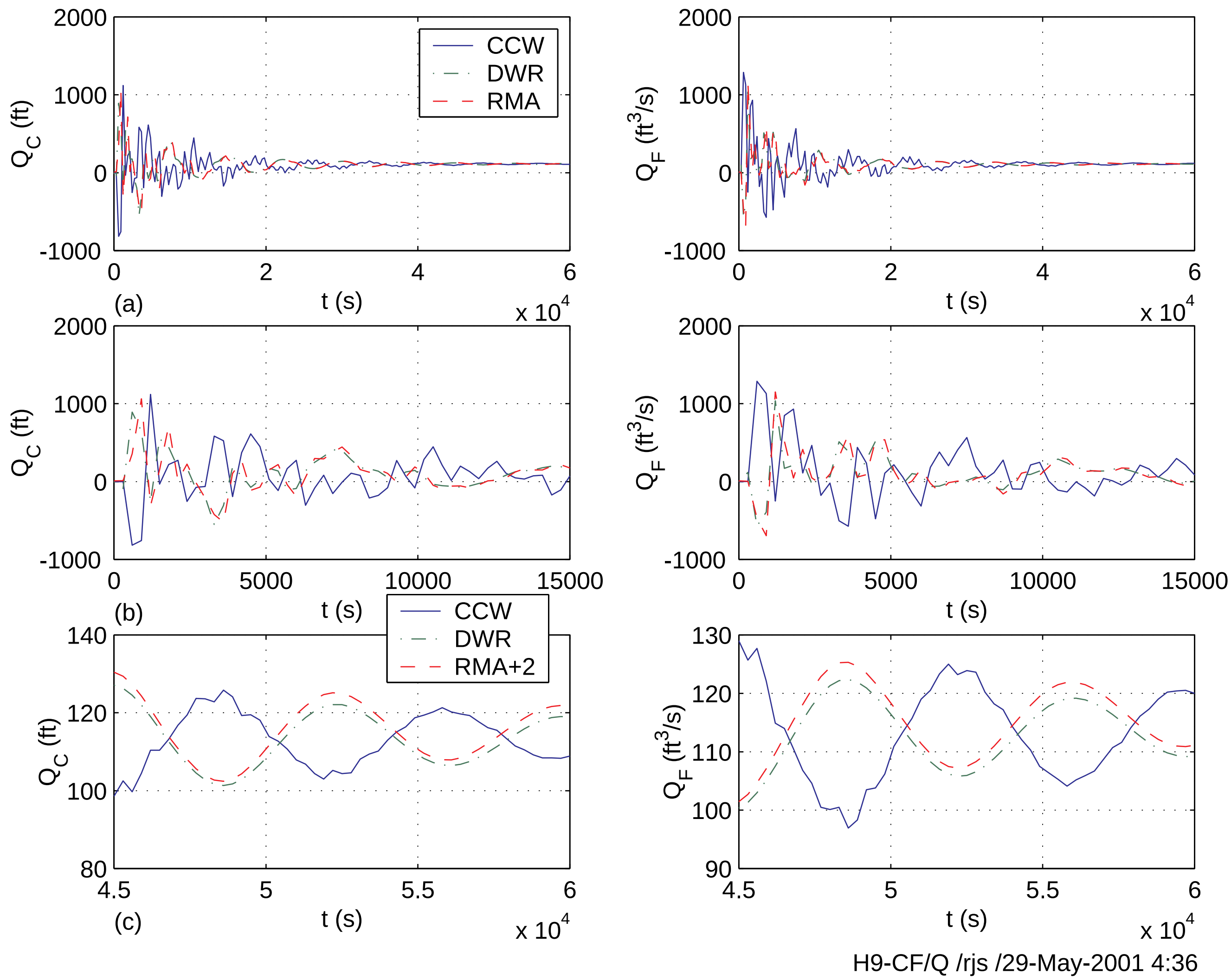

Figure 12.14: Flow evolution at Nodes C and F in Reach CF.